

Article

Energy Consumption Prediction and Analysis for Electric Vehicles: A Hybrid Approach






Hamza Mediouni, Amal Ezzouhri, Zakaria Charouh, Khadija El Harouri, Soumia El Hani
and Mounir Ghogho



<https://doi.org/10.3390/en15176490>

Article

Energy Consumption Prediction and Analysis for Electric Vehicles: A Hybrid Approach

Hamza Mediouni ^{1,2,*} , Amal Ezzouhri ^{2,3} , Zakaria Charouh ^{2,3} , Khadija El Harouri ¹, Soumia El Hani ¹  and Mounir Ghogho ^{2,4} 

¹ Energy Optimization, Diagnosis and Control Team, Center for Research in Engineering and Health Sciences and Techniques, ENSAM, Mohammed V University, Rabat 10100, Morocco

² TICLab, College of Engineering & Architecture, International University of Rabat, Rabat 11100, Morocco

³ ERSC Team, Mohammadia Engineering School, Mohammed V University, Rabat 10090, Morocco

⁴ School of EEE, University of Leeds, Leeds LS2 9JT, UK

* Correspondence: hamza_mediouni@um5.ac.ma or hamza.mediouni@uir.ac.ma

Abstract: Range anxiety remains one of the main hurdles to the widespread adoption of electric vehicles (EVs). To mitigate this issue, accurate energy consumption prediction is required. In this study, a hybrid approach is proposed toward this objective by taking into account driving behavior, road conditions, natural environment, and additional weight. The main components of the EV were simulated using physical and equation-based models. A rich synthetic dataset illustrating different driving scenarios was then constructed. Real-world data were also collected using a city car. A machine learning model was built to relate the mechanical power to the electric power. The proposed predictive method achieved an R^2 of 0.99 on test synthetic data and an R^2 of 0.98 on real-world data. Furthermore, the instantaneous regenerative braking power efficiency as a function of the deceleration level was also investigated in this study.

Keywords: range anxiety; hybrid approach; synthetic dataset; real-world data; instantaneous regenerative braking power



Citation: Mediouni, H.; Ezzouhri, A.; Charouh, Z.; El Harouri, K.; El Hani, S.; Ghogho, M. Energy Consumption Prediction and Analysis for Electric Vehicles: A Hybrid Approach. *Energies* **2022**, *15*, 6490. <https://doi.org/10.3390/en15176490>

Academic Editor: Byoung Kuk Lee

Received: 5 July 2022

Accepted: 23 July 2022

Published: 5 September 2022

Publisher's Note: MDPI stays neutral with regard to jurisdictional claims in published maps and institutional affiliations.



Copyright: © 2022 by the authors. Licensee MDPI, Basel, Switzerland. This article is an open access article distributed under the terms and conditions of the Creative Commons Attribution (CC BY) license (<https://creativecommons.org/licenses/by/4.0/>).

1. Introduction

Over the last few decades, there has been an increase in greenhouse gas (GHG) emissions from various sectors, owing to the usage of fossil fuels. The majority of the emissions are ascribed to vehicles that rely on fossil fuel in their internal combustion engines. On the other hand, the limited minable reserves of fossil fuels and their imbalanced distribution have also led to global energy crises during the last century [1]. To overcome this crisis, governments and international communities around the world have been pushing to adopt sources of clean energy. Electric vehicles (EVs) are considered as an option to achieve a low-carbon transportation system. In many countries around the globe, ambitious targets have been set to promote EVs [2], and some even aim to ban the sale of internal combustion engine vehicles in the not-so-distant future [3].

Despite the EV's environmental benefits, and the government's incentives, their market penetration and widespread adoption are affected by the high purchase cost, limited charging station infrastructure, high charging time, and limited driving range. Indeed, one of the main issues associated with the use of EVs is the so-called range anxiety problem [4]. To mitigate this issue, an accurate prediction of the driving range estimate is required, in addition to increasing battery capacity and densifying the network of charging stations.

The estimation of the remaining driving range requires both the evaluation of the battery's remaining energy and the prediction of the future energy consumption. Several factors affect the energy consumption of an EV, which can be divided into two main categories: internal factors and external ones [5]. Internal factors are related to the vehicle itself, including vehicle characteristics, vehicle components efficiency, and auxiliary devices

usage. The battery system is one of the core components of an EV. Its technical features have a significant influence on energy consumption, as does the regeneration rate, which is dependent on vehicle technology, vehicle speed, acceleration, state of charge, and other factors. Other vehicle-related factors include motor and drive-train efficiency, as well as the vehicle's mass, frontal area, drag coefficient, and the rolling resistance which varies depending on tire pressure and design. The heating, ventilation and air-conditioning (HVAC) system is also considered as a relevant factor; its impact on energy consumption is largely determined by the local environment and the driver's thermal comfort preferences [6,7]. Other auxiliary components include lighting, power steering, radio, navigation system, and other comfort-related devices, which are powered by a low-voltage battery supplied by the traction battery; the total impact of these components on energy consumption is rather small compared to other components [8]. External Factors associated with driving conditions include environmental and traffic conditions, road type and topography, driving behavior, etc. The natural environmental factors include the weather, especially wind speed and its orientation due to the resulting aerodynamics forces, ambient temperature, and humidity due to their impact on the use of HVAC systems. The topography can be characterized by different parameters, one of which is the road's slope angle. In general, the slope gradient has a remarkable effect on the maximum driving range and route planning [9,10]. Indeed, positive slopes increase energy consumption while negative slopes may help restore some energy to the traction battery. Furthermore, the driver's behavior, which is attributed to several characteristics depending on age, gender, attitude, etc., affects considerably the energy consumption. Indeed, the more aggressive the driving style, the higher the variations in acceleration and deceleration, and the average speed. The traffic conditions also affect the overall energy consumption; these are generally characterized by the levels of congestion or traffic flows.

EVs' energy consumption estimation models can be classified into three main categories: analytical, statistical, and computational models [11]. Analytical models are based on longitudinal vehicle dynamics and powertrain efficiencies [12,13]. Longitudinal vehicle dynamics are modeled from the vehicle dynamics theory to calculate the required power at the wheels to propel the vehicle. The model developed in [14] took into consideration the efficiency of all powertrain components instead of that of the motor only. In [15], the model expressed the relationship between EV speed, acceleration, power, and road grade to determine the required power at the wheels. The model could be used to estimate the "instantaneous" energy consumption over a trip for ecoroute planning. In [5], a power-based EV energy consumption model was developed using a real EV, including its powertrain system, longitudinal vehicle dynamics, transmission, battery model, and auxiliary devices. The model was validated using the given driving cycles and energy consumption values found in the literature. Furthermore, a regenerative braking strategy was developed to model the real braking controller behavior.

Statistical models are based on real-world driving data to understand and deduce empirical relationships between an EV's energy consumption and different factors affecting consumption. For example, in [16], a systematic energy consumption estimation approach based on historical and real-world driving condition data collected from typical urban travel routes was developed in order to derive polynomial combinations of an EV's instantaneous speed, acceleration, and battery state of charge under different driving modes. In [17], by using the information on traffic situations, driving style, road features, and environmental variables, multiple linear regression (MLR) models were built to find and quantify correlations between the kinematic parameters of the vehicle and its energy use. Each model aggregated input parameters at a different level, allowing predictions to be made using a variety of input values. In [11], a data-driven energy consumption decomposition analysis was conducted by investigating two newly constructed compound factors: negative kinetic energy (NKE), and positive kinetic energy (PKE). To demonstrate the usefulness of these two components, the prediction model was built on this decomposition and feature selection analysis.

Computational models based on artificial neural networks (ANN) were developed to estimate the relationship between an EV's energy consumption and factors affecting consumption [11,18]. Having a learning ability, this type of model can be used as a function of the input factors, where each factor is associated with weights depending on its relative importance [11]. ANNs can be used also to predict driving behavior by classifying driving patterns using real-world driving data. The adoption of an estimation approach depends on data availability and the targeted application. Analytical models require less computational effort than statistical and computational models, but the latter are generally more accurate since they are data-driven. Some references employ hybrid methods that combine physics-based and data-driven approaches to make use of each method, as is the case with an Argonne National Laboratory simulation program called "Autonomie" [19]. This simulator is based on data analysis and vehicle parameters and has demonstrated good accuracy against test data.

This work aims to predict an EV's energy consumption under real-world driving conditions by taking into account different exogenous and endogenous factors. For this purpose, an EV model is designed using MATLAB/Simulink software based on a real EV, Renault's Zoe Q210. The EV model comprises longitudinal vehicle dynamics and the vehicle powertrain system. The driver model is developed to control the vehicle's speed and to realistically represent a human driver's behavior. The storage system model is parameterized using the battery datasheet including the rated capacity, the number of cells in series/parallel, initial battery capacity, and other parameters. The electric motor and drive electronics are designed using mapped motor and drive electronics operating in torque-control mode. Furthermore, the longitudinal vehicle dynamics is designed to model the overall required power at the wheels as a function of the kinematic parameters describing vehicle movement. The EV's energy consumption simulator is used to illustrate different driving scenarios in order to construct a synthetic dataset including the mechanical power at the wheels as well as the required power from the battery to drive the vehicle. The constructed mechanical power is calculated using synthetic speed profiles and synthetic driving conditions, covering all possible cases of slope angle, road topography, additional load, and wind speed. The vehicle under test is monitored using an Android application measuring and recording data from the vehicle controller area network (CAN) using an on-board controller (OBD). The CAN data provide information in the form of the required force and torque at the wheels, vehicle speed, battery current, and battery voltage. In the acceleration mode, the real-world measurements are used to test the machine learning model trained with the synthetic dataset. Moreover, in the deceleration mode, the experimental data are used to determine the instantaneous regenerative braking function when releasing the accelerator pedal with and without using the braking system, as well as to determine the regenerative braking power efficiency as a function of deceleration level at the end. The remaining sections of this paper are organized as follows. The EV's model is described in Section 2. Section 3 provides a taxonomy of the factors affecting energy consumption and a description of standard driving cycles. The methodology used to construct the synthetic dataset is explained in Section 4. The proposed energy consumption model is described in Section 5, along with the presentation and discussion of the simulation results. Conclusions are drawn in Section 6.

2. Vehicle Modeling

The Renault Zoe Q210 was considered here for the EV modeling as a case study. This was based on this EV's technical specifications, cost, and availability in our region. The vehicle specifications are presented in Table 1.

Table 1. Electric vehicle specifications.

Parameters	Value
Curb weight	1468 kg
Battery capacity	22 kWh
Motor power	65 kW
Maximum velocity	135 km/h
Battery weight	275 kg
Frontal area	2.14 m ²
Maximum torque	220 N.m
Drag coefficient	0.35
Wheel radius	0.3105 m

The modeling was implemented using MATLAB/Simulink software and comprised the different subsystems listed below.

2.1. Driver Model

The driver model aimed to emulate the human driver's behavior. Modeling driving behavior is a difficult task because it depends on many subjective factors. In this study, a simplified driver model was considered. This consisted in minimizing the error (e_v) between the drive cycle (reference desired speed, $V_{desired}$) and the actual vehicle's speed V_{actual} . Depending on the sign of the error, the driver either accelerates or decelerates to force the vehicle to follow the reference speed profile: when (e_v) is positive, an acceleration command is generated, whereas, when (e_v) is negative, the driver has two options: either release only the accelerator pedal to slow down the vehicle or press the brake pedal to slow down the vehicle using the frictions brakes. In this study, a proportional–integral (PI) controller was chosen to model the driver's behavior; the command, in the Laplace domain, was modeled as follows:

$$C_{PI}(s) = P + \frac{I}{s} \quad (1)$$

where P and I are the proportional and integral gains, respectively, and s is the Laplace variable.

2.2. Braking Strategy Model

The maximum available force to decelerate the vehicle, depending on the adhesion between the tires and the road, and the normal load acting on the vehicle, can be expressed as [20]:

$$F_{B_{MAX}} = \phi(Z_f + Z_r) = \phi M_{veh}g \quad (2)$$

where ϕ is the adhesion coefficient between the tires and the road, Z_f and Z_r are the normal loads on the front and rear axles in Newtons, respectively, M_{veh} is the vehicle mass in kg and g is the acceleration due to gravity in m/s². Typical values of ϕ are around 0.8 on concrete surfaces and on dry or wet asphalt.

2.3. Electric Motor and Drive Electronics Model

In this study, a mapped motor and drive electronics operating in the torque-control mode were used to reduce the simulation time; the user can specify the maximum motor power and torque or mechanical torque range with a torque–speed envelope. The torque demand was the input of the electric motor model, whereas the motor torque was the model's output computed by taking into account motor and inverter efficiencies. The torque demand T_{Dem} was derived from the driver model as follows:

$$T_{Dem} = T_{Max}D_{acc} \quad (3)$$

where T_{Max} is the maximum available torque in N and D_{acc} is the driver's acceleration command in a percentage from 0 to 100.

2.4. Battery Model

The implemented battery model was based on discharge characteristics taken at different temperatures. The model could be parameterized through experimental measurements or using a typical battery datasheet. The advantage of this model was that it could be used for different electric vehicle batteries and customized using lookup tables for the battery's open-circuit voltage and the internal resistance. The lookup tables were functions of the state of charge and battery temperature. Further, the user can modify the number of cells in series/parallel, rated capacity, initial battery capacity, and other parameters. The battery model input was the total current demand for propulsion, and auxiliary devices, which took into account energy losses along the powertrain. Furthermore, the outputs of the model were the battery terminal voltage, current, state of charge obtained using the following equations:

$$V_{\text{Bat}} = V_{\text{Cell}} N_s \quad (4)$$

$$I_{\text{Bat}} = I_{\text{Cell}} N_p \quad (5)$$

$$SOC_t = SOC_i - \frac{\int_a^b I_{\text{cell}}(\tau) d\tau}{C_{\text{cell}}} \quad (6)$$

where N_s and N_p are the number of cells in series and in parallel, respectively, V_{mcell} and V_{Bat} are the single cell and the battery pack terminal voltage in V , I_{cell} and I_{Bat} are the single cell and the battery pack's current in A , SOC_t is the battery state of charge in (%), SOC_i is the initial battery state of charge in (%), C_{cell} is the single cell capacity in Ah , and I_{Cell} is the single cell current demand in A .

2.5. Driveline and Transmission Model

The aim of the transmission system is to transfer the torque between the motor and the driving wheels. The efficiency of the transmission system affects the EV's energy consumption and it is defined in traction mode as follows:

$$\eta_{\text{Tr}} = \frac{T_w \omega_w}{T_m \omega_m} \quad (7)$$

where ω_w and ω_m are the wheels and the motor speed, respectively, in rad/s and T_m and T_w are the motor torque and the torque at the driving wheels in Nm .

2.6. Auxiliary Devices Model

The power consumed by the auxiliary devices can affect considerably the total energy consumption. These are powered by a 12 V battery that is charged via a DC/DC converter by the high-voltage battery pack. The power demand of auxiliary devices can be calculated as follows:

$$P_{\text{dem}} = \frac{P_{\text{aux}}}{\eta_c \eta_{\text{bat}}} \quad (8)$$

where P_{dem} is the power demand in W , P_{aux} is the power consumption of the auxiliary devices in W , and η_c and η_{bat} are the efficiencies of the DC/DC converter and the 12 V battery, respectively.

2.7. Longitudinal Vehicle Dynamics

The overall required power at the wheels as a function of the kinematic parameters describing the vehicle movement can be expressed as follows:

$$P_{\text{mechanical}} = (F_i + F_{\text{aero}} + F_{\text{rr}} + F_{\text{gr}}) V_{\text{veh}} \quad (9)$$

where F_i is the resistance force inertia related to the forces required for the linear acceleration of the vehicle described as:

$$F_i = Ma, \quad (10)$$

F_{aero} is the aerodynamic drag force due to the friction between the air and the vehicle body described as:

$$F_{\text{aero}} = \frac{1}{2} \rho A C_D (V_{\text{veh}}^2 + V_w^2), \quad (11)$$

F_{rr} is the rolling resistance force due to the friction between the tires and the road defined as:

$$F_{\text{rr}} = Mg C_{\text{rr}} \cos(\theta), \quad (12)$$

and F_{gr} represents the resistance force due to the road inclination with regard to the horizontal plane defined as:

$$F_{\text{gr}} = Mg \sin(\theta). \quad (13)$$

In the above equations, M is the vehicle mass in kg, a is the vehicle acceleration in m/s^2 , ρ is the air density in kg/m^3 , A is the vehicle frontal area in m^2 , C_D is the drag coefficient, V_{veh} is the vehicle speed in m/s , and V_w is the wind speed, g is the acceleration due to gravity m/s^2 , C_{rr} is the coefficient of rolling resistance, and θ is the inclination angle of the road in $^\circ$.

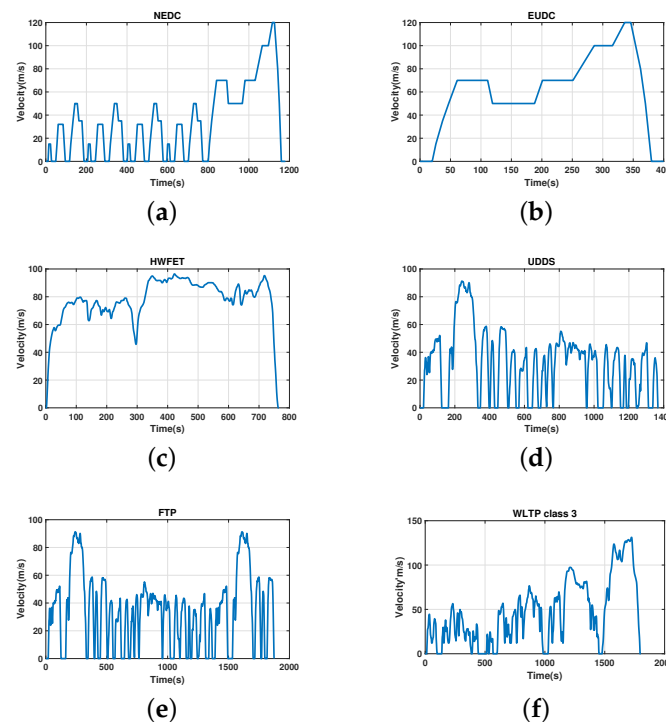
3. Standard Driving Cycles and Factors Impacting Energy Consumption

3.1. Standard Driving Cycles

A driving cycle is a velocity–time profile used to describe the characteristics of a vehicle in a specific traffic environment [21]. Each drive cycle is constructed for a specific road structure, driver behavior, and traffic flow characteristics to evaluate energy consumption, driving range, and equivalent emissions of an electric vehicle [22,23]. Since the beginning of the 1970s, many countries and regions have given great importance to the development of driving cycles and established strict regulations [24]. The New European Driving Cycle (NEDC), last updated in 1997, is designed to evaluate the emission levels of car engines and fuel economy in passenger cars. It excludes light trucks and commercial vehicles. The test offers a stylized driving-speed pattern with low accelerations, constant speed cruises, and many idling events. The Extra Urban Driving Cycle (EUDC) is a part of NEDC which accounts for more aggressive, high-speed driving modes. The maximum speed in a EUDC is 120 km/h and its duration is 400 s. The Highway Fuel Economy Test (HWFET or HFET) cycle is a chassis dynamometer driving schedule developed by the US Environmental Protection Agency (EPA) for the determination of fuel economy of light-duty vehicles. It is used to determine the highway fuel economy rating and its duration is 765 s. The US FTP-72 (Federal Test Procedure) cycle, also called the Urban Dynamometer Driving Schedule (UDDS) test, is designed to assess fuel economy. It is used for light-duty vehicle testing. The cycle simulates an urban route of 12.07 km with frequent stops. The maximum speed is 91.25 km/h and the average speed is 31.5 km/h. The Federal Test Procedure (FTP) is composed of the UDDS followed by the first 505 s of the UDDS. It is often called the EPA75. The dynamometer portion of the test procedure has a very complex timeline of events including the cold start phase, transient phase, and hot start phase. The World Harmonized Light-Duty Vehicles Test Procedure (WLTP) is a globally harmonized standard for determining fuel consumption, the levels of CO_2 emissions of traditional and hybrid cars, as well as the range of fully electric vehicles. The WLTP Class 3 is divided into four different subparts, each one with a dissimilar maximum speed, to simulate urban, suburban, rural, and highway scenarios, with an equal division between urban and nonurban paths. The characteristics of the discussed drive cycles are given in Table 2, and their velocity time profiles are depicted in Figure 1, where (a), (b), (c), (d), (e) and (f) refer respectively to NEDC, UDDS, HWFET, UDDS, FTP and WLTP class 3.

Table 2. Standard driving cycles characteristics.

Characteristics	NEDC	EUDC	HWFET	UDDS	FTP	WLTP C3
Duration(s)	1160	400	765	1369	1874	1800
Distance(km)	11.2	6.95	16.51	11.99	17.77	23.26
Max speed (km/h)	120	120	96.4	91.24	91.24	131
Average speed (km/h)	33.57	62.28	77.47	31.48	34.09	46.47
Max Acceleration (m/s^2)	1.04	0.69	1.43	1.47	1.47	1.75

**Figure 1.** Velocity time profile of some standard driving cycles. (a) NEDC; (b) UDDS; (c) HWFET; (d) UDDS; (e) FTP; (f) WLTP Class 3.

3.2. Factors Impacting Energy Consumption

Numerous factors can impact the energy consumption of an electric vehicle. They can be classified as exogenous and endogenous factors. Endogenous elements are related to vehicle characteristics and driver behavior, whereas exogenous factors cover all the natural and artificial environments. Temperature, wind speed and orientation, precipitation, road topography, climate zone, and others can be grouped into the natural environment, whilst traffic flow, congestion level, and road type can refer to the artificial environment.

3.2.1. Vehicle Technology Factors

The battery system is the core of the electric vehicle propulsion system. Its specifications, including the used chemicals, energy density, capacity, number of cells and modules, regeneration rate, and state of health, affect the overall energy consumption. The vehicle's auxiliaries, and in particular the HVAC system, are also considered as significant factors in its energy consumption due to the absence of a combustion engine [25]. Further, the vehicle's curb weight and additional mass have an influence on energy consumption mainly when climbing hills and at starting torque. The vehicle's frontal area determines the aerodynamic resistive force which affects directly the energy consumption. Other vehicle-related factors are the powertrain system and the motor efficiency, and the rolling resistance referred to as tire pressure and design [9].

3.2.2. Driver Behavior

A driver is associated with different attributes including age, gender, attitude, etc. [26]. Aggressive driving, which is characterized by a high variability in the acceleration and deceleration driving patterns [25,27], is associated with a higher energy consumption [28]. Further, the desired thermal comfort may vary amongst drivers, which implies that energy consumption due to the use of the HVAC system may depend on the driver. Other factors impacting the energy consumption are the physical conditions of the driver and the psychology of range anxiety [29].

3.2.3. Climatic Conditions

Climatic conditions have a direct impact on the vehicle's driving range. Customers reported up to a 40% decrease in the driving range on hot summer and/or cold winter days compared to the maximum range [30]. This reduction is particularly pronounced in cold weather conditions. Indeed, cold temperatures negatively impact the energy consumption for two main reasons: electric cabin cooling consumes less power compared to heating [31] and batteries require self-heating when the ambient temperature is low. Furthermore, wind speed and orientation affect the energy consumption, and this impact provides additional incentives for reducing the aerodynamic drag of electric vehicles.

3.2.4. Road Topography

Road gradients have a remarkable effect on the maximum driving range and route planning [32,33]. Upward gradients lead to an increased energy consumption while downward gradients help to restore the energy back to the battery with the use of the regenerative braking system. The force associated with a downward gradient can be described as:

$$F_{gr} = Mg \sin(\theta) \quad (14)$$

3.2.5. Road Conditions

Road conditions are considered as external factors impacting driving efficiency. Increasing traffic volume and congestion generally lead to a higher energy consumption due mainly to higher rates of use of the HVAC system as journeys take longer [34].

4. Synthetic Dataset Construction Methodology

The overall mechanical energy at the wheels as a function of the kinematic parameters can be expressed as:

$$E_{ij} = \int_{t_i}^{t_j} P_{\text{mechanical}}(t) dt \quad (15)$$

where E_{ij} is, respectively, the mechanical energy required at the wheels from time instant t_i to time instant t_j . For the construction of the dataset, energy values corresponded to one second, i.e., $t_j - t_i = 1$ s.

4.1. Synthetic Speed Profile Construction

Any speed profile can be approximated by a piecewise linear function where each segment/piece can be represented by an initial value (i.e., initial speed), and a slope (acceleration). We used this idea to construct synthetic time–speed drive cycles to cover different driving conditions scenarios (acceleration, deceleration, and cruise). Figure 2 depicts the speed profile references, and Table 3 illustrates the acceleration and initial speed ranges.

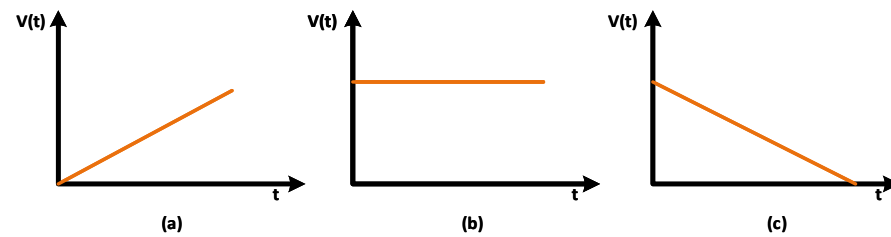


Figure 2. Synthetic speed profile construction: (a) Acceleration; (b) Cruising; (c) Deceleration .

Table 3. Initial speed and acceleration ranges variation.

Parameters	Minimum	Maximum	Step
V_0 (km/h)	0	120	20
a (m/s ²)	−3.5	2.5	0.5

To represent the real driving conditions, many factors were taken into consideration in the construction of the dataset. In this study, wind speed, slope angle, road topography, and additional load were considered.

The maximum speed allowed by the vehicle was 135 km/h. The maximum acceleration was that corresponding to a variation of the speed from 0 to 100 km/h in 13.5 s. The speed profile ranges were therefore chosen to be within these limits. The wind speed variations were chosen based on historical data in our region. Different slope angle values were considered. The additional mass variations were selected according to the maximum mass authorized by the vehicle. The coefficient of rolling resistance values were chosen to mimic the tread patterns and road states assuming that the tires' pressure was properly set. Table 4 illustrates the range of different parameters.

Table 4. Internal and external parameters variation ranges variation.

Parameters	Minimum	Maximum	Step
V_w (m/s)	0	40	10
θ (°)	−9	9	3
C_{rr}	0	0.08	0.02
m (kg)	1468	1968	100

In acceleration mode, the initial vehicle speed was set to zero and then incremented by 20 km/h until it reached the maximum speed of the vehicle. In cruising mode, the acceleration was set to zero and the initial vehicle speed was set to 20 km/h and incremented by 20 km/h until it reached the maximum allowed value. In deceleration mode, the initial vehicle was set at the maximum authorized value and then decreased by 20 km/h until it reached the value of zero. Figures 3–5 depict the synthetic acceleration, cruising, and deceleration profiles, respectively.

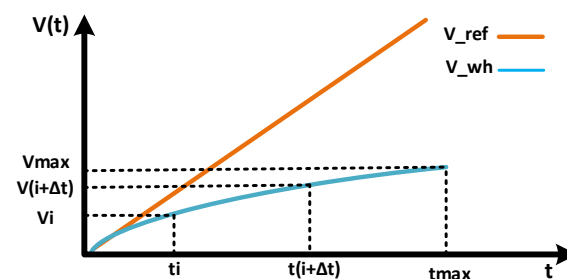


Figure 3. Synthetic acceleration profile.

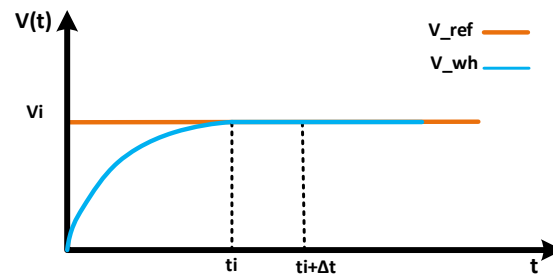


Figure 4. Synthetic cruise profile.

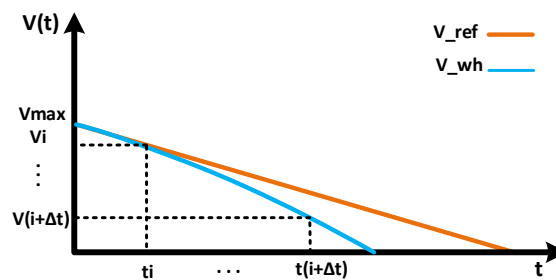


Figure 5. Synthetic deceleration profile.

4.2. Synthetic Dataset Construction

The main objective of the dataset construction was to build a model to predict the energy consumption of the Q210 Renault Zoe Model on any given road by taking into consideration exogenous and endogenous parameters including driving behavior, road conditions, natural environment, and additional weight. The inputs were acceleration, initial speed, slope angle, additional mass, wind speed, and coefficient of rolling resistance; the outputs were the required mechanical power at the wheels and the equivalent electric power to drive the vehicle. The parameters taken into consideration in this study are described in Table 5.

Table 5. Factors impacting energy consumption used for dataset construction.

Parameter	Designation	Factor
V_{vh}	Vehicle speed	Driver behavior
a	Vehicle acceleration	Driver behavior
θ	Slope angle	Road topography
C_{rr}	Coefficient of rolling resistance	Road topology
m	Additional mass	Vehicle Characteristics
V_w	Wind speed	Climatic conditions

5. Proposed Energy Consumption Model

The proposed energy consumption model was a combination of a physics-based model and a machine learning model. The mechanical power at the wheels was calculated using Equation (15). The mapping between the required mechanical power and the required electric power was estimated using a machine learning model, which was built to characterize the different interactions between the storage system, the powertrain, and the propulsion system. The machine learning model was trained using the constructed dataset. The schematic overview of the proposed hybrid model is presented in Figure 6.

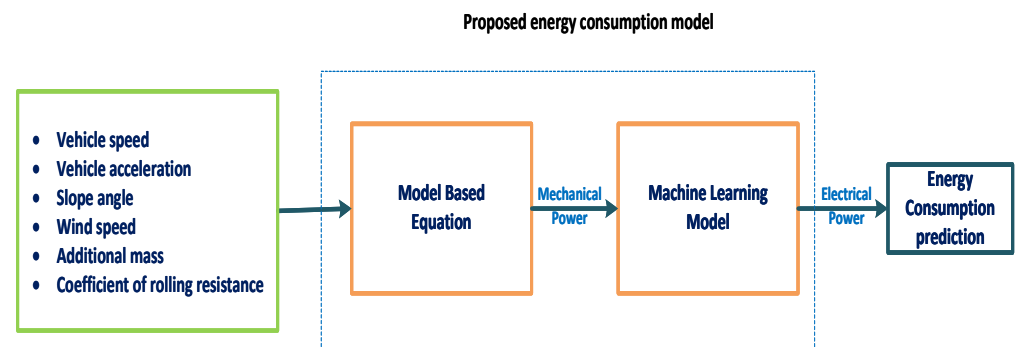


Figure 6. Schematic overview of the proposed energy consumption prediction model.

5.1. Real-World Measurement

The vehicle under test was monitored using an Android application that collected data from the vehicle controller area network (CAN) using an on-board controller (OBD). The CAN data provided information on the vehicle's speed, required force at the wheels, battery voltage, and battery current.

An example of the tests conducted for this study is depicted in Figure 7. It illustrates the vehicle's speed, required force at the wheels, battery voltage, and battery current (from top to bottom). The tests were performed for disparate levels of acceleration, deceleration, and different states of charge. In the acceleration mode, the vehicle's speed and the required force at the wheels increased to reach the maximum mechanical power, whereas the battery voltage and current decreased to attain the maximum battery discharge current. In the deceleration mode, the vehicle speed decreased until the vehicle achieved the idling mode and the required force at the wheels changed direction to decelerate the engine. Furthermore, the battery voltage gradient was incremented, and the current changed sign to charge the battery.

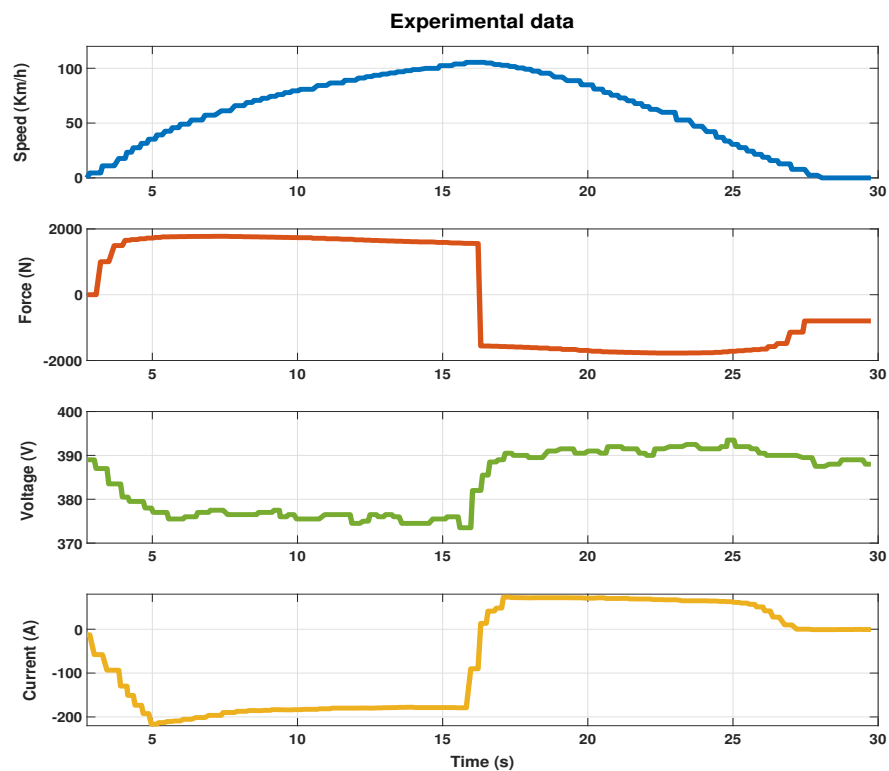


Figure 7. Data collected from vehicle CAN bus: vehicle speed, required force at the wheels, battery voltage, and battery current (from top to bottom).

Figures 8–10 illustrate the relationship between the storage system power and power at the wheels in the traction and regeneration modes. In the traction mode, the energy flows from the motor to the wheels. In this case, the power at the wheels is assumed to be positive due to the fact that the power at the electric motor is higher than the power at the wheels. In addition, the required power from the battery to drive the vehicle is assumed to be negative (see Figure 8). On the other hand, in the regenerative braking mode, energy flows from the wheels to the motor. In this case, the power at the wheels is higher than the power at the electric motor. Thus, it is assumed to be negative and the recovered power by the battery is considered positive. In our study, regenerative braking could be performed by acting on the braking pedal (see Figure 9), or by releasing the accelerator pedal where the vehicle was in the freewheel mode (see Figure 10).

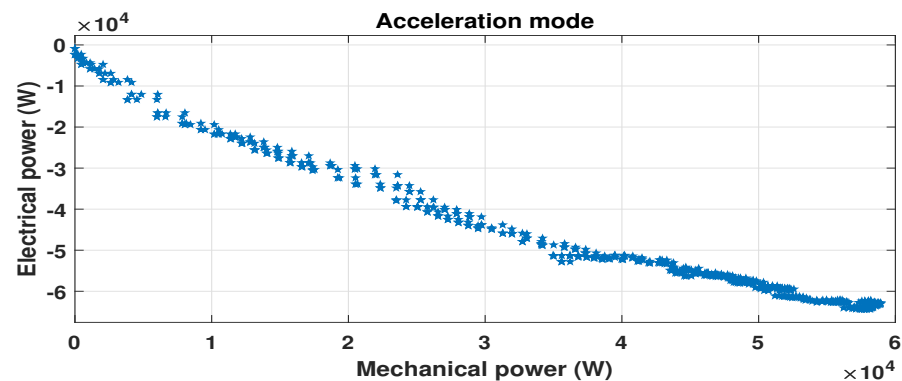


Figure 8. Efficiency of electric vehicle in acceleration mode.

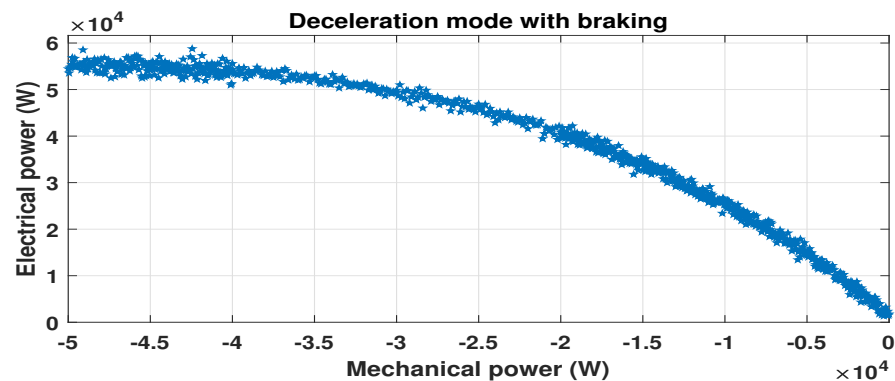


Figure 9. Efficiency of electric vehicle in deceleration mode with using braking system.

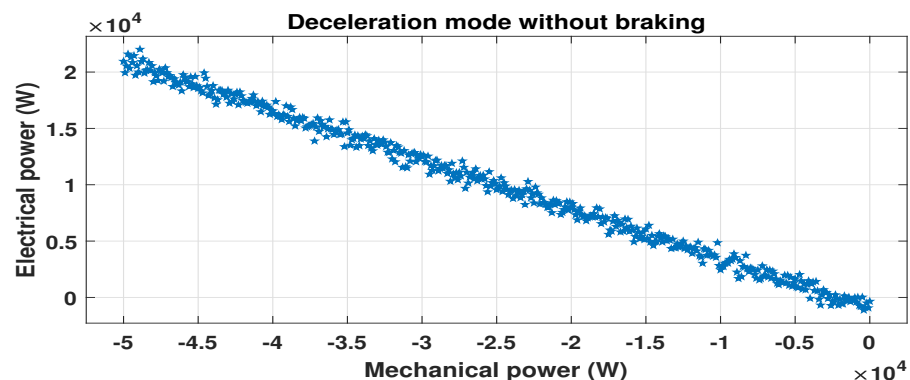


Figure 10. Efficiency of electric vehicle in deceleration mode without using braking system.

5.2. Machine Learning Models

5.2.1. Acceleration Mode

In the acceleration mode, the machine learning model was built using the synthetic dataset: 70% (respectively, 30%) of the data were used to train (respectively, test) the model. As mentioned above, the coefficients of the machine learning model vary with the settings of the physical models of the vehicle. These settings were then adjusted to fit real-world data using curve fitting. Figure 11 depicts the battery power as a function of the mechanical power while using real measurements, and Table 6 showcases the performance of the model tested on synthetic and real measurements data.

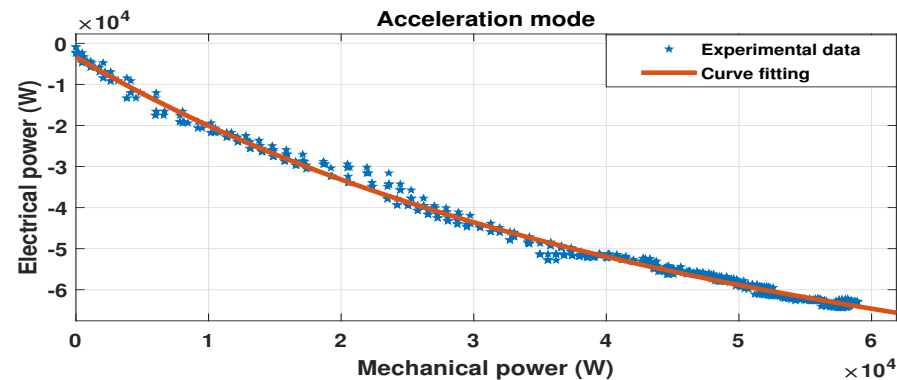


Figure 11. Battery power as a function of mechanical power in acceleration mode.

Table 6. Performance of elaborated model on both datasets.

Dataset	R-Square	RMSE (W)
Synthetic dataset	0.9954	716.14
Real-world measurements	0.9824	856.08

5.2.2. Deceleration Mode

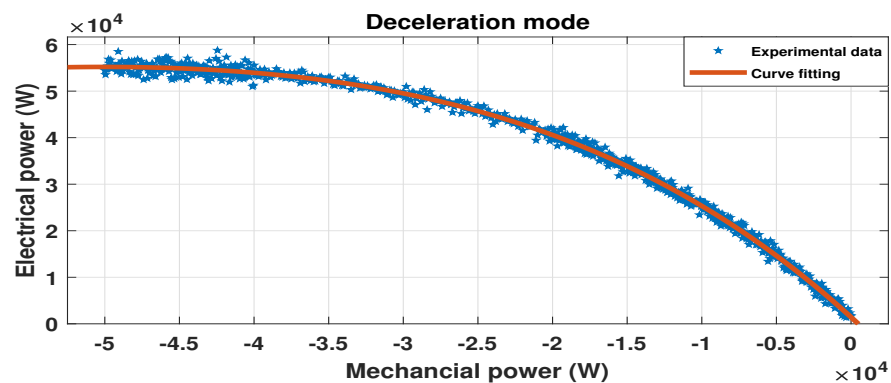
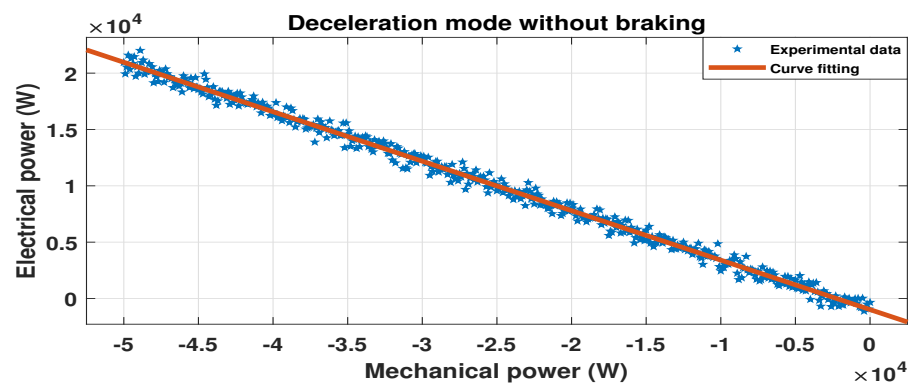
The correlation between the mechanical power at the wheels and the required electrical power to drive the vehicle in acceleration and deceleration mode with the use of the braking system can be expressed by:

$$P_{\text{electric}} = k_1 e^{k_2 P_{\text{mechanical}}} + k_3 e^{k_4 P_{\text{mechanical}}} \quad (16)$$

The above equation represents a two-term exponential curve-fitting model whose parameters were obtained using a nonlinear least squares method based on a trust-region algorithm. The maximum number of iterations was set to 600 and the tolerance function was set to 1.0×10^{-6} . Moreover, in the case of deceleration without using the braking pedal, the relationship between the mechanical and the electrical power was approximately linear, i.e., $P_{\text{electric}} = k_5 P_{\text{mechanical}} + k_6$. The coefficients and the performance of each model are given in Table 7, where the R-square and root-mean-square error (RMSE) were used as metrics to assess the goodness of fit. Figures 12 and 13 illustrate the curve fitting functions in deceleration mode with and without using the braking system, respectively.

Table 7. Coefficients and performance of elaborated models.

Driving State	Coefficients (with 95% Confidence Bounds)	R-Square	RMSE (W)
Deceleration (with braking)	$k_1 = -2.754 \times 10^4$ ($-2.826 \times 10^4, -2.682 \times 10^4$) $k_2 = 0.0001613$ (0.0001518, 0.0001708) $k_3 = 2.494 \times 10^4$ $(2.423 \times 10^4, 2.565 \times 10^4)$ $k_4 = -2.765 \times 10^{-6}$ ($-3.51 \times 10^{-6}, -2.02 \times 10^{-6}$)	0.9955	547.4
Deceleration (without braking)	$k_5 = -0.4419$ ($-0.4422, -0.4417$) $k_6 = -1356$ ($-1363, -1350$)	0.9999	58.58

**Figure 12.** Battery power as a function of mechanical power in deceleration mode with braking.**Figure 13.** Battery power as a function of mechanical power in deceleration mode without braking.

5.3. Regenerative Braking Power Efficiency as a Function of Deceleration

The efficiency of the EV powertrain in deceleration mode depends on the level and the duration of deceleration and on the use of the braking pedal. In the case of changing the braking pedal position, the efficiency of the powertrain in regenerative mode can be expressed by an exponential function for different levels of deceleration, whereas the simple linear regression can be used to express the relationship between the mechanical and electrical power in the case of decelerating by releasing only the accelerator pedal. Based on experimental measurements of regenerative braking power values and using curve fitting as well as concatenation of the two modes of deceleration, the instantaneous regenerative braking was found to be well approximated by

$$\eta = k_7 e^{k_8 a} + k_9 e^{k_{10} a} \quad (17)$$

In the above equation, a nonlinear least squares method was adopted using a trust-region algorithm, where the maximum number of iterations and the tolerance function

were set, respectively, to 600 and 1.0×10^{-6} . η refers to the regenerative braking efficiency, a is the instantaneous acceleration, which is negative in this case, and k_7 , k_8 , k_9 , and k_{10} are coefficients whose values are given in Table 8, which also shows the performance of the proposed curve fitting in terms of R^2 and the root-mean-square error (RMSE). Figure 14 illustrate the variation in the instantaneous regenerative braking efficiency as a function of the deceleration level.

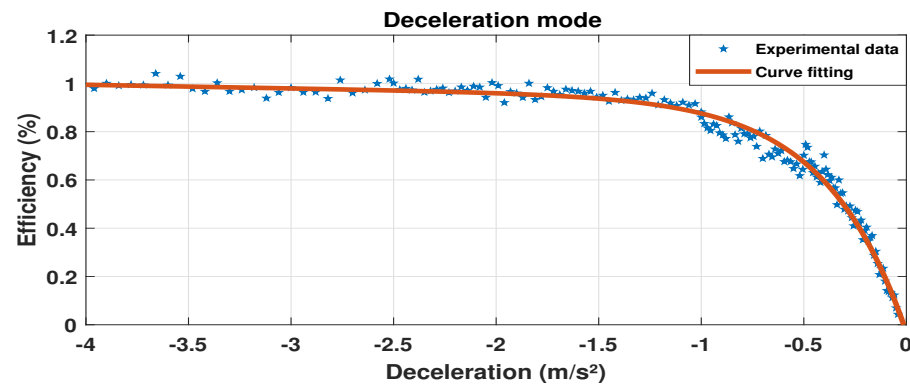


Figure 14. Variation in the instantaneous regenerative braking efficiency as a function of the deceleration level.

5.4. Results and Discussion

Extensive simulations showed that in the acceleration mode (i.e., $a \geq 0$), a good mapping between the mechanical power and the electric power was obtained with a sum of two exponentials. The values of the parameters of these two exponentials changed with the settings of the physical models' coefficients (e.g., driveline and transmission model). Real data confirmed this modeling as described before. In the deceleration mode, real data showed that the regenerated electric power was a linear function of the mechanical power in the absence of braking and a sum of two exponentials in the presence of braking. Based on experimental measurements, and by concatenating the two modes of deceleration, the instantaneous regenerative braking efficiency as a function of deceleration level was found to be approximated using a two-term exponential decay function. The results in Tables 7 and 8 show that the proposed models performed well in terms of R^2 and root-mean-square error (RMSE).

Table 8. Coefficients and performance of the instantaneous regenerative braking efficiency as a function of the deceleration level.

Coefficients (with 95% Confidence Bounds)	R-Square	RMSE (%)
$k_7 = 0.9645$ (0.8555, 1.073)	0.9785	0.0548
$k_8 = -0.009234$ (−0.05018, 0.03171)		
$k_9 = -1.036$ (−1.149, −0.9221)		
$k_{10} = 2.848$ (2.006, 3.69)		

6. Conclusions

In this work, we proposed a hybrid approach to predict EV's energy consumption under real-world driving conditions. Different exogenous and endogenous factors were taken into account. These included driving behavior, road conditions, natural environment, and additional weight. The proposed energy consumption simulator, which included the vehicle's powertrain system and longitudinal vehicle dynamics, was used to construct a synthetic dataset. The latter, along with real-world data, was used to determine the relationship between the mechanical power at the wheels and the electric power in both acceleration and deceleration modes. Furthermore, the instantaneous regenerative braking energy efficiency as a function of the deceleration level was investigated in this study. This

EV's energy consumption model can be updated using real-world data to quantify the degradation of powertrain components. Furthermore, it can be beneficial to automotive decision-makers for the optimal sizing of components such as battery and powertrain and to EV drivers for route planning to alleviate range anxiety.

Author Contributions: Conceptualization, H.M. and M.G.; Data curation, H.M. and A.E.; Formal analysis, H.M., A.E. and Z.C.; Funding acquisition, S.E.H. and M.G.; Investigation, H.M. and Z.C.; Methodology, H.M., A.E. and Z.C.; Project administration, S.E.H. and M.G.; Resources, S.E.H. and M.G.; Software, K.E.H.; Supervision, S.E.H. and M.G.; Validation, H.M., A.E., Z.C., S.E.H. and M.G.; Visualization, H.M. and K.E.H.; Writing—original draft, H.M.; Writing—review & editing, S.E.H. and M.G. All authors have read and agreed to the published version of the manuscript.

Funding: This work was partly funded through RSK-E-Mobility project by the Moroccan region of Rabat-Salé-Kenitra (RSK).

Conflicts of Interest: The authors declare no conflict of interest. The funders had no role in the design of the study; in the collection, analyses, or interpretation of data; in the writing of the manuscript, or in the decision to publish the results.

References

- Genikomsakis, K.N.; Mitrentsis, G. A computationally efficient simulation model for estimating energy consumption of electric vehicles in the context of route planning applications. *Transp. Res. Part D Transp. Environ.* **2017**, *50*, 98–118. [\[CrossRef\]](#)
- Shankar, R.; Marco, J. Method for estimating the energy consumption of electric vehicles and plug-in hybrid electric vehicles under real-world driving conditions. *IET Intell. Transp. Syst.* **2013**, *7*, 138–150. [\[CrossRef\]](#)
- Salvucci, R.; Tattini, J. Global outlook for the transport sector in energy scenarios. In *DTU International Energy Report 2019: Transforming Urban Mobility*; DTU: Denmark, 2019; pp. 21–27.
- De Cauwer, C.; Verbeke, W.; Coosemans, T.; Faïd, S.; Van Mierlo, J. A data-driven method for energy consumption prediction and energy-efficient routing of electric vehicles in real-world conditions. *Energies* **2017**, *10*, 608. [\[CrossRef\]](#)
- Miri, I.; Fotouhi, A.; Ewin, N. Electric vehicle energy consumption modelling and estimation—A case study. *Int. J. Energy Res.* **2021**, *45*, 501–520. [\[CrossRef\]](#)
- Petrauskiene, K.; Dvarionienė, J.; Kaveckis, G.; Kliugaite, D.; Chenadec, J.; Hehn, L.; Pérez, B.; Bordi, C.; Scavino, G.; Vignoli, A.; et al. Situation analysis of policies for electric mobility development: Experience from five European regions. *Sustainability* **2020**, *12*, 2935. [\[CrossRef\]](#)
- Pollák, F.; Vodák, J.; Soviar, J.; Markovič, P.; Lentini, G.; Mazzeschi, V.; Luè, A. Promotion of electric mobility in the European Union—Overview of project PROMETEUS from the perspective of cohesion through synergistic cooperation on the example of the catching-up region. *Sustainability* **2021**, *13*, 1545. [\[CrossRef\]](#)
- Cerdas, F. *Integrated Computational Life Cycle Engineering for Traction Batteries*; Springer: Cham, Switzerland, 2022.
- Ritzmann, J.; Chinellato, O.; Hutter, R.; Onder, C. Optimal Integrated Emission Management through Variable Engine Calibration. *Energies* **2021**, *14*, 7606. [\[CrossRef\]](#)
- Treeyakarn, P.; Sooklamai, M.; Jiracheewanun, S.; Meearsa, J. Performance analysis of an electric car when using different battery types. *J. Res. Appl. Mech. Eng.* **2021**, 1–11. [\[CrossRef\]](#)
- Qi, X.; Wu, G.; Boriboonsomsin, K.; Barth, M.J. Data-driven decomposition analysis and estimation of link-level electric vehicle energy consumption under real-world traffic conditions. *Transp. Res. Part Transp. Environ.* **2018**, *64*, 36–52. [\[CrossRef\]](#)
- Croce, A.I.; Musolino, G.; Rindone, C.; Vitetta, A. Traffic and energy consumption modelling of electric vehicles: parameter updating from floating and probe vehicle data. *Energies* **2021**, *15*, 82. [\[CrossRef\]](#)
- Zhao, G.; Wang, X.; Negnevitsky, M. Connecting Battery Technologies for Electric Vehicles from Battery Materials to Management. *iScience* **2022**, *25*, 103744. [\[CrossRef\]](#) [\[PubMed\]](#)
- Szumaska, E.M.; Jurecki, R.S. Parameters influencing on electric vehicle range. *Energies* **2021**, *14*, 4821. [\[CrossRef\]](#)
- Fiori, C.; Ahn, K.; Rakha, H.A. Power-based electric vehicle energy consumption model: Model development and validation. *Appl. Energy* **2016**, *168*, 257–268. [\[CrossRef\]](#)
- Koengkan, M.; Fuinhas, J.A.; Belucio, M.; Alavijeh, N.K.; Salehnia, N.; Machado, D.; Silva, V.; Dehdar, F. The Impact of Battery-Electric Vehicles on Energy Consumption: A Macroeconomic Evidence from 29 European Countries. *World Electr. Veh. J.* **2022**, *13*, 36. [\[CrossRef\]](#)
- De Cauwer, C.; Van Mierlo, J.; Coosemans, T. Energy consumption prediction for electric vehicles based on real-world data. *Energies* **2015**, *8*, 8573–8593. [\[CrossRef\]](#)
- Ai, Y.; Li, J.; Yu, H.; Liu, Y. Real-road energy consumption characteristics of electric passenger car in China: A case study in Shenzhen. In *IOP Conference Series: Earth and Environmental Science, Proceedings of the 2019 3rd International Conference on Power and Energy Engineering, Qingdao, China, 25–27 October 2019*; IOP Publishing: Bristol, UK, 2020; Volume 431, p. 012064.

19. Islam, E.; Moawad, A.; Kim, N.; Rousseau, A. *An Extensive Study on Sizing, Energy Consumption, and Cost of Advanced Vehicle Technologies*; Contract ANL/ESD-17/17; Argonne National Laboratory (ANL): Argonne, IL, USA, 2018.
20. Dik, A.; Omer, S.; Boukhanouf, R. Electric Vehicles: V2G for Rapid, Safe, and Green EV Penetration. *Energies* **2022**, *15*, 803. [[CrossRef](#)]
21. Brady, J.; O'Mahony, M. Development of a driving cycle to evaluate the energy economy of electric vehicles in urban areas. *Appl. Energy* **2016**, *177*, 165–178. [[CrossRef](#)]
22. Zhao, X.; Ye, Y.; Ma, J.; Shi, P.; Chen, H. Construction of electric vehicle driving cycle for studying electric vehicle energy consumption and equivalent emissions. *Environ. Sci. Pollut. Res.* **2020**, *27*, 37395–37409. [[CrossRef](#)] [[PubMed](#)]
23. Sun, D.J.; Zheng, Y.; Duan, R. Energy consumption simulation and economic benefit analysis for urban electric commercial-vehicles. *Transp. Res. Part Transp. Environ.* **2021**, *101*, 103083. [[CrossRef](#)]
24. Liu, B.; Shi, Q.; He, L.; Qiu, D. A study on the construction of Hefei urban driving cycle for passenger vehicle. *IFAC-PapersOnLine* **2018**, *51*, 854–858. [[CrossRef](#)]
25. Li, W.; Stanula, P.; Egede, P.; Kara, S.; Herrmann, C. Determining the main factors influencing the energy consumption of electric vehicles in the usage phase. *Procedia Cirp* **2016**, *48*, 352–357. [[CrossRef](#)]
26. Gebisa, A.; Gebresenbet, G.; Gopal, R.; Nallamotheu, R.B. Driving Cycles for Estimating Vehicle Emission Levels and Energy Consumption. *Future Transp.* **2021**, *1*, 615–638. [[CrossRef](#)]
27. Petersen, P.; Khdar, A.; Sax, E. Feature-Based Analysis of the Energy Consumption of Battery Electric Vehicles. In Proceedings of the 7th International Conference on Vehicle Technology and Intelligent Transport Systems VEHITS, Online Streaming, 28–30 April 2021; pp. 223–234.
28. Wróblewski, P.; Kupiec, J.; Drożdż, W.; Lewicki, W.; Jaworski, J. The Economic Aspect of Using Different Plug-In Hybrid Driving Techniques in Urban Conditions. *Energies* **2021**, *14*, 3543. [[CrossRef](#)]
29. Thatcher, A.; Yeow, P.H. *Ergonomics and Human Factors for a Sustainable Future*; Springer: Singapore, 2018.
30. Tal, G.; Karanam, V.C.; Favetti, M.P.; Sutton, K.M.; Ogunmayin, J.M.; Raghavan, S.S.; Nitta, C.; Chakraborty, D.; Davis, A.; Garas, D. *Emerging Technology Zero Emission Vehicle Household Travel and Refueling Behavior*; eScholarship, UC Davis Institute of Transportation Studies: Davis, CA, USA, 2021.
31. Vora, A.P.; Jin, X.; Hoshing, V.; Shaver, G.; Varigonda, S.; Tyner, W.E. Integrating battery degradation in a cost of ownership framework for hybrid electric vehicle design optimization. *Proc. Inst. Mech. Eng. Part D J. Automob. Eng.* **2019**, *233*, 1507–1523. [[CrossRef](#)]
32. Gaete-Morales, C.; Kramer, H.; Schill, W.P.; Zerrahn, A. An open tool for creating battery-electric vehicle time series from empirical data, emobpy. *Sci. Data* **2021**, *8*, 1–18. [[CrossRef](#)]
33. Liu, K.; Yamamoto, T.; Morikawa, T. Impact of road gradient on energy consumption of electric vehicles. *Transp. Res. Part Transp. Environ.* **2017**, *54*, 74–81. [[CrossRef](#)]
34. Gorcun, O.F. Reduction of energy costs and traffic flow rate in urban logistics process. *Energy Procedia* **2017**, *113*, 82–89. [[CrossRef](#)]